Large magnetostriction in Fe-based alloys predicted by density functional theory

Y. N. Zhang and R. Q. Wu
Department of Physics and Astronomy, University of California, Irvine, California 92697-4575, USA
(Received 21 August 2010; revised manuscript received 11 October 2010; published 15 December 2010)

Through systematic density functional calculations using the full potential linearized augmented plane-wave method, extraordinary large magnetostrictions are found in Fe-based alloys with appropriate mixing of metalloid and 5*d* element. For instance, tetragonal magnetostrictive coefficients of $Fe_{87.5}Pt_{6.25}Ga_{6.25}$ and $Fe_{75}Pt_{6.25}Ge_{18.75}$ in their model structures can reach to +943 ppm and −3553 ppm, respectively. This was assigned to the availability of nonbonding states around the Fermi level and the large spin-orbit coupling of 5*d* atoms. The effects of distribution patterns of 5*d* and metalloid elements and their hybridization are discussed to provide insights for further experimental explorations.

DOI: 10.1103/PhysRevB.82.224415 PACS number(s): 75.80.+q, 71.15.Mb, 71.20.Be, 75.30.Gw

I. INTRODUCTION

Extensive fundamental investigations on magnetic systems greatly promote the development of new functional materials that are needed for technological innovations.[1–3] The magnetostriction is one of the most important features of new materials for exploitations in sensors, actuators, transducers, microelectromechanical system (MEMS),[4,5] and also in the innovative energy converting devices. Recently, it has been demonstrated in several prototype material systems that magnetization, magnetic ordering, and spin dynamics of complex materials can be controlled by applying electric field.[6–8] This offers new ways toward making efficient spintronic devices with "zero current" operation on magnetic units. Effective conversion between electric and magnetic energies has also been achieved using magnetostrictive-piezoelectric composites through mechanical strains.[9] $Fe_{100-x}Ga_x$ (Refs. 10 and 11) alloys, which exhibit enhanced tetragonal magnetostrictive coefficient up to 400 ppm, are very promising magnetostrictive materials for this type applications. Extensive interdisciplinary efforts have been dedicated to understand the mechanism of the extraordinary enhancement of magnetostriction in these alloys[12–15] and to lay a foundation for the rational design of better magnetostrictive materials.[5,16,17]

Recent *ab initio* studies indicate that the intrinsic change in electronic structures induced by Ga plays an essential role in the large magnetostriction of $Fe_{100-x}Ga_x$ alloys.[15,18] Several factors, including spin polarization of Fe, spin-orbit coupling (SOC), availability of electronic states around Fermi level, as well as electron population, may significantly affect the magnetostriction of Fe-based alloys. In this paper, we introduce 5*d* elements into the Fe-based alloys to test if we can further enhance magnetostriction with their large SOC. By combining different factors, as sketched in Fig. 1, we found that many ternary alloys can possess giant magnetostriction, i.e., $|\lambda_{001}| > 1000$ ppm, very promising for practical applications.

II. COMPUTATIONAL DETAILS

Density functional calculations were performed using the full potential linearized augmented plane-wave method.[19] The core electrons were treated fully relativistically while the spin-orbit coupling term was invoked second variationally for the valence states.[20] No shape approximation was assumed for charge, potential, and wave-function expansions. The spin-polarized generalized gradient approximation was adopted for the description of exchange-correlation interactions among electrons.[21] Energy cutoffs of 225 Ry and 16 Ry were chosen for the charge potential and basis expansions in the interstitial region, respectively. In the muffin-tin region ($r_{Fe}=1.11$ Å, $r_{Pt}=1.38$ Å, and $r_{Ga}=1.22$ Å), charge, potential, and basic functions were expanded in terms of spherical harmonics with a maximum angular momentum of $l_{max}=8$. Self-consistence was assumed when the root-mean-square differences between the input and output charge and spin densities are less than 1.0×10^{-4} $e/(\text{a.u.})^3$.

The tetragonal magnetostrictive coefficient λ_{001} was determined through the following equation:[20]

$$\lambda_{001} = \frac{2dE_{MCA}/d\varepsilon}{3d^2E_{tot}/d\varepsilon^2}, \tag{1}$$

where ε is the tetragonal strain applied along the z axis (in the constant-volume mode); E_{MCA} and E_{tot} are magnetocrystalline anisotropy and total energies of alloys, respectively. We adopted the torque approach[20] for the determination of E_{MCA}. For the $(2\times2\times2)$ cubic supercell (16 atoms/cell), we used 1800 k points to sample the irreducible Brillouin zone (BZ). Further increase in k point up to 4200 only change the value of E_{MCA} by $<1\%$. Lattice sizes and atomic positions were optimized according to the energy minimization procedure guided by atomic forces with a criterion that atomic force on each atom is less than 0.01 eV/Å.

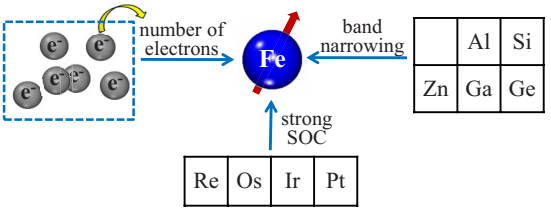

FIG. 1. (Color online) Schematic of the key factors for the increase in magnetostriction in Fe-based alloys.

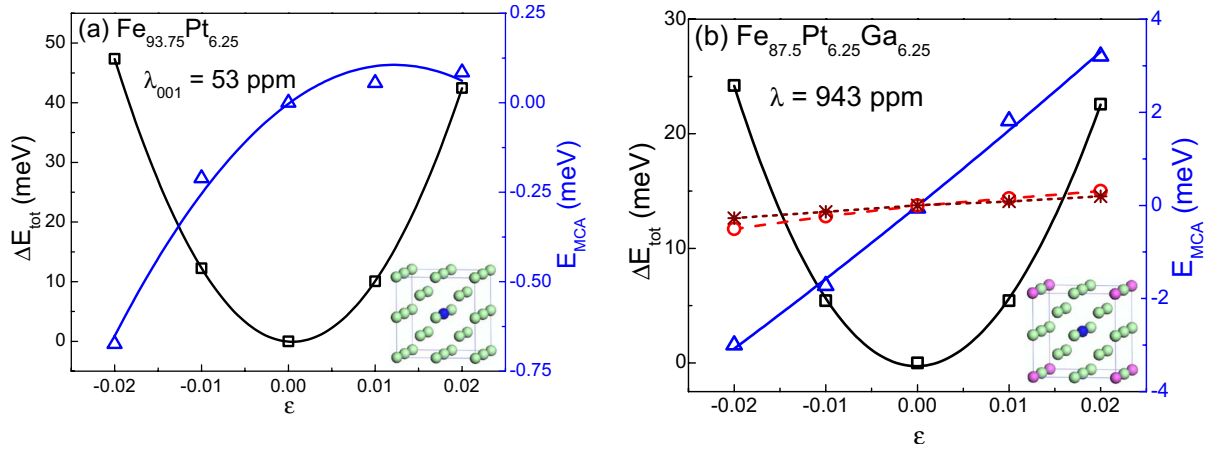

FIG. 2. (Color online) The total energy E_{tot} (open squares) and magnetocrystalline anisotropy energy E_{MCA} (open triangles) of $Fe_{93.75}Pt_{6.25}$ and $Fe_{87.5}Pt_{6.25}Ga_{6.25}$ as a function of lattice strain along the z axis. The open circles (asterisks) with dashed (short-dashed) line in (b) represent the strain dependence of E_{MCA} of $Fe_{87.5}Ga_{12.5}$ ($Fe_{93.75}Ga_{6.25}$). The insets are the atomic configurations used in the calculations, where green (light gray), blue (dark), and pink (gray) spheres denote Fe, Pt, and Ga atoms, respectively.

III. RESULTS AND DISCUSSIONS

From Eq. (1), one may find that the most crucial factor for the design of highly magnetostrictive materials is to have large magnetoelastic coupling: $dE_{MCA}/d\varepsilon$. According to the quantum-mechanical perturbation theory,[22]

$$E_{MCA} = \sum_{o,u} \frac{[\langle o|\xi L_z|u\rangle^2 - \langle o|\xi L_x|u\rangle^2]}{E_o - E_u}, \tag{2}$$

where o and u denote occupied and unoccupied electronic states; E_o and E_u are their energies; L_z and L_x are the angular momentum operators; ξ is the strength of SOC. Naturally, we should look for alloys with large ξ to enhance the numerator[23,24] and rich electronic states around the Fermi level (E_F) to reduce the denominator.[25] Pt is chosen as the provider of large SOC in the present studies because it is also benign to magnetization of Fe as found in perpendicular magnetic recording media.[26] As sketched in insets of Fig. 2, we place one Pt atom at the center of the 16-atom unit cell so the Pt concentration is fixed at 6.25%. We found that the Pt atom has a large spin moment, 0.46–0.47 μ_B. Meanwhile, the magnetic moment of the adjacent Fe(C) atoms[27] also increases to 2.53 μ_B, from typical values of 2.2–2.3 μ_B in alloys without Pt.

From results of the strain-dependent E_{MCA} and E_{tot} presented in Fig. 2(a), we found that the magnetostrictive coefficient λ_{001} of $Fe_{93.75}Pt_{6.25}$ is only +53 ppm. This value is in line with experimental data for FePt random alloys at this composition ratio but is certainly far from adequate for most applications. The weak magnetoelastic response of $Fe_{93.75}Pt_{6.25}$ was found to stem from the absence of appropriate electronic states around the Fermi level. Curves of density of states (DOS) in Figs. 3(a) and 3(b) clearly suggest that the number of states at E_F (or $E=0$) is very low for both Fe and Pt atoms in $Fe_{93.75}Pt_{6.25}$. According to Eq. (2), large energy separation between occupied and unoccupied states results in small magnetic anisotropy and magnetostriction.

Adding Ga into the system should change this situation since Ga atoms in the Fe lattice break Fe-t_{2g} bonds. We started with one Ga atom in the cell (6.25%) and placed it at a large distance away from Pt, shown in the inset of Fig. 2(b). Comparing the DOS curves of $Fe_{93.75}Pt_{6.25}$ and $Fe_{87.5}Pt_{6.25}Ga_{6.25}$ alloys in Figs. 3(a) and 3(b), we found that Ga brings in nonbonding states near E_F in the minority-spin channel and purges small amount of holes of $Fe_{93.75}Pt_{6.25}$ in the majority-spin channel. The energy sliced charge density in Fig. 3(c) for states within ±0.2 eV indicates that the Ga-induced nonbonding peaks near E_F mainly comprise of Fe(C)-t_{2g} and Pt-e_g features. Due to the weak Fe-Ga hybridization, Fe(C)-$d_{xz,yz}$ states no longer extend far toward the adjacent Ga sites and become "dangling" bonds. It is striking to find that λ_{001} of $Fe_{87.5}Pt_{6.25}Ga_{6.25}$ becomes unusually high, +943 ppm, a value which is even 2–3 times higher than the best magnetostrictive coefficient of Fe-Ga alloys reported so far. This indicates a possibility of making strongly magnetostrictive materials through combined actions of Pt which provides large spin-orbit coupling, and Ga (or other metalloid elements) which weakens the d states of Fe(C). With the same configuration model, the calculated λ_{001} of $Fe_{87.5}Pt_{6.25}Al_{6.25}$ is also as high as +1156 ppm.

The importance of large SOC of Pt on λ_{001} is clearly demonstrated in Fig. 2(b), where the strain dependences of E_{MCA} of $Fe_{87.5}Pt_{6.25}Ga_{6.25}$, $Fe_{93.75}Ga_{6.25}$, and $Fe_{87.5}Ga_{12.5}$ are given together. While the calculated E_{MCA} of the distorted $Fe_{87.5}Pt_{6.25}Ga_{6.25}$ structure ($\varepsilon=2\%$) is over 3 meV/cell, the corresponding values of Fe-Ga binary alloys are only ~0.45 meV/cell. In addition, E_{MCA} and also λ_{001} of $Fe_{87.5}Pt_{6.25}Ga_{6.25}$ drop by a factor of 7 if we selectively switch off the SOC of Pt in calculations. Another factor for the increase in magnetostriction is that the addition of Ga or other metalloid elements significantly softens the lattice. For instance, the tetragonal shear modulus C' reduces from 57 GPa in $Fe_{93.75}Pt_{6.25}$ to 34 GPa in $Fe_{87.5}Pt_{6.25}Ga_{6.25}$. Another example for the need of combining the effects of large SOC and weak bonds is for $Fe_{93.75}Ir_{6.25}$ and $Fe_{87.5}Ir_{6.25}Al_{6.25}$ model structures: the magnitude of λ_{001} of $Fe_{87.5}Ir_{6.25}Al_{6.25}$ (+178 ppm) is six times higher than that of $Fe_{93.75}Ir_{6.25}$ (−28 ppm).

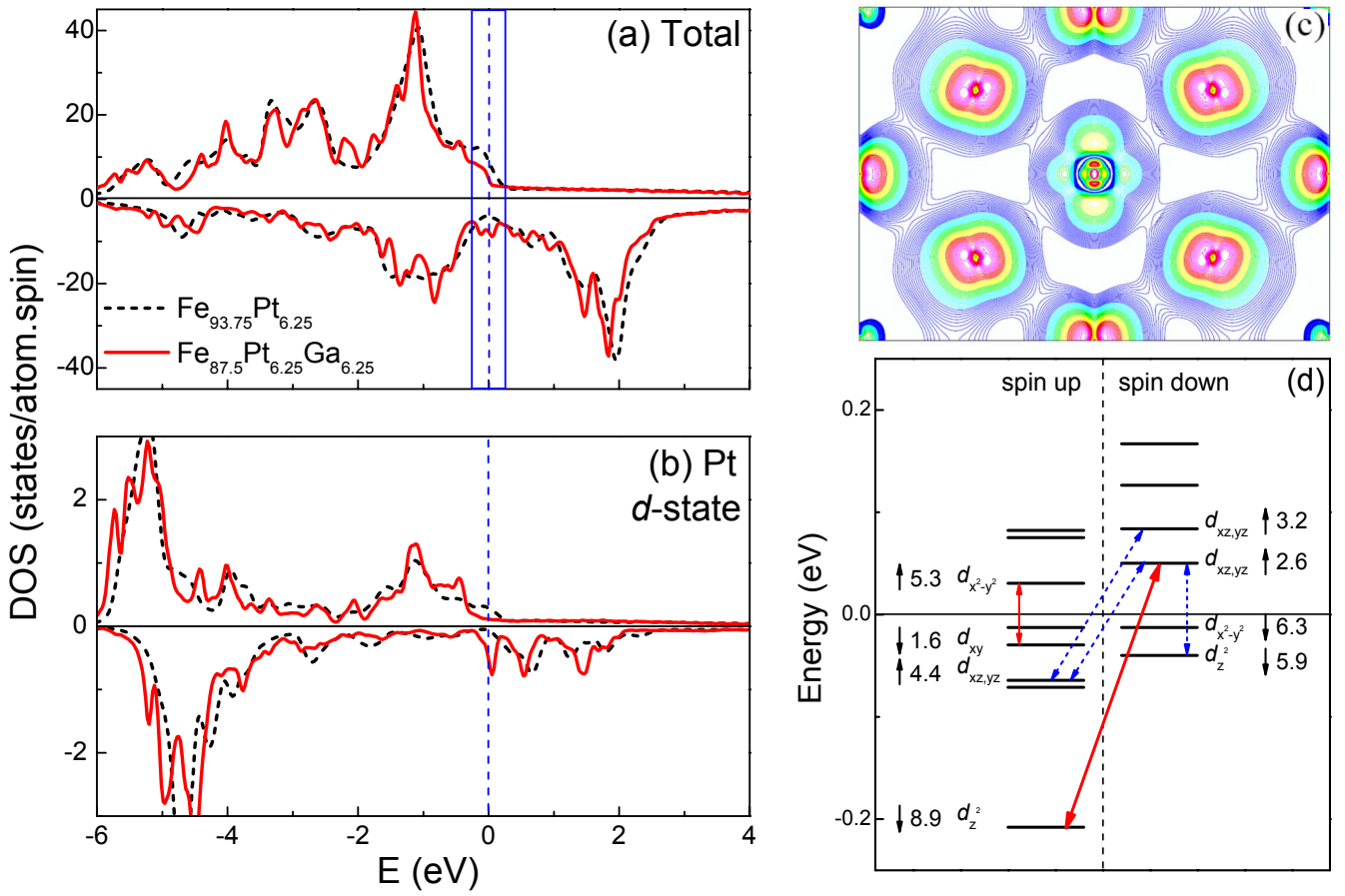

FIG. 3. (Color online) Calculated (a) total density of states and (b) projected density of states in the Pt atom of $Fe_{93.75}Pt_{6.25}$ and $Fe_{87.5}Pt_{6.25}Ga_{6.25}$ alloys. Positive and negative values are for the majority and minority spins, respectively. Zero energy is the position of the Fermi level. (c) Energy-sliced charge density of $Fe_{87.5}Pt_{6.25}Ga_{6.25}$ (± 0.2 eV around E_F). (d) Eigenvalues near the Fermi level and their wave-function features and strain-induced shifts of $Fe_{87.5}Pt_{6.25}Ga_{6.25}$ at the Γ point. The solid and dashed arrows highlight the key pairs of states that make positive and negative contributions to E_{MCA}, respectively.

We performed detailed studies of the distribution of $E_{MCA}(\varepsilon)$ in the BZ as we did for other systems[28] and identified that the most active region in BZ is around the $\bar{\Gamma}\bar{X}$ line for the $Fe_{87.5}Pt_{6.25}Ga_{6.25}$ structure. To appreciate roles of different electronic states, we give all eigenstates near the Fermi level (± 0.2 eV) at the $\bar{\Gamma}$ point in Fig. 3(d), and highlight the key pairs of occupied and unoccupied states. In addition to the Fe(C)-$d_{xz,yz}$ states, we also found two e_g orbitals in this energy range. As shown by arrows, the d_{z^2} states in both the majority- and minority-spin channels play the key role in producing large enhancement of E_{MCA}, mainly through the $\langle xz\downarrow|\xi L_x|z^2\downarrow\rangle$ and $\langle xz\downarrow|\xi L_x|z^2\uparrow\rangle$ couplings across the Fermi level (the up and down arrows denote the majority and minority spins, respectively). Because of strong mixing between Fe(C)-d and Pt-d_{z^2} states, as seen in Fig. 3(b), these matrix elements are much larger than those in binary Fe-Ga alloys. Moreover, the energy positions of these states, i.e., E_o and E_u in Eq. (2), are sensitive to the tetragonal lattice distortions since the d_{z^2} states point along the (001) axis. Quantitatively, the direction and magnitude of strain-induced energy shifts are also given in Fig. 3(d) for different d states around the Fermi level.[29] It is obvious that eigenenergies of the d_{z^2} states change much faster (about 2 times) than other states under lattice distortions.

To explore if adding more Ga atoms can further enhance λ_{001}, we also investigated the $Fe_{75}Pt_{6.25}Ga_{18.75}$ alloy. There are two possible arrangements that keep the cubic symmetry of the 16-atom unit cell, namely, the $B2$-like and $D0_3$-like. Nevertheless, the $D0_3$-like structure is unstable under the tetragonal distortion, thus we only focus on results of the $B2$-like structure depicted in the inset of Fig. 4. Surprisingly, the strain dependence of E_{MCA} given in Fig. 4 is rather weak and the value of λ_{001} is only +222 ppm. Although the addition of Ga generates plenty nonbonding states around the Fermi level of $Fe_{75}Pt_{6.25}Ga_{18.75}$, it does not lead to large magnetostriction. To see the reason of this unexpected decrease, we plotted the band filling (N_e) dependence of E_{MCA} for $Fe_{75}Pt_{6.25}Ga_{18.75}$ under two opposite strains ($\varepsilon = \pm 2\%$) in the inset of Fig. 4, using a rigid-band approach.[15] We found that the actual Fermi level lies close to the nodes of the $E_{MCA}(N_e)$ curves, resulting in a small slope of the $E_{MCA}(\varepsilon)$ curve. However, it's possible to drastically enhance λ_{001} if we can manage to move the Fermi level to $N_e = 148-150$ electrons/cell, as marked by the vertical dashed line in the inset of Fig. 4. Practically, this is doable by replacing Ga with Ge (Ref. 30 that has similar behavior toward hybridizing with Fe atoms but provides one more itinerant electron per atom. Indeed, the calculated $E_{MCA}(\varepsilon)$ curve of $Fe_{75}Pt_{6.25}Ge_{18.75}$ displays a

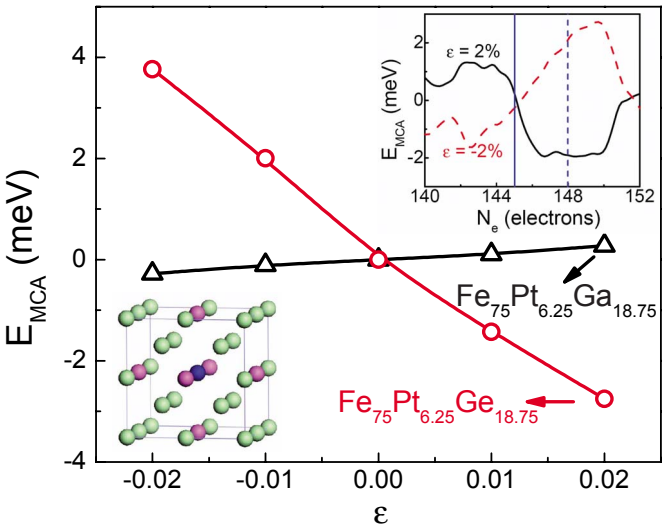

FIG. 4. (Color online) Calculated $E_{MCA}(\varepsilon)$ of $Fe_{87.5}Pt_{6.25}Ga_{6.25}$ and $Fe_{87.5}Pt_{6.25}Ge_{6.25}$. The lower left inset gives the atomic configuration. The upper right inset shows the calculated E_{MCA} against the band filling, N_e, for $Fe_{87.5}Pt_{6.25}Ga_{6.25}$ with +2% and −2% lattice distortions along the z axis. The solid and dashed vertical lines in the upper right inset present the positions of Fermi levels of $Fe_{87.5}Pt_{6.25}Ga_{6.25}$ and $Fe_{87.5}Pt_{6.25}Ge_{6.25}$, respectively.

much steep negative slope compared to that of $Fe_{75}Pt_{6.25}Ga_{18.75}$. The amplitude of λ_{001} of this hypothetical $Fe_{75}Pt_{6.25}Ge_{18.75}$ structure is astonishingly high, 3500 ppm, even much larger than that of Terfenol-D [$\lambda_{111} \sim 1600$ ppm (Ref. 31)]. The rigid-band model is also held good in other Fe-5d alloys. The E_{MCA}-N_e curves of $Fe_{75}Pt_{6.25}Al_{18.75}$ indicate that by adjusting the N_e to ~118 electrons/cell, i.e., to substitute Al by Si atoms, the calculated λ_{001} of $Fe_{75}Pt_{6.25}Si_{18.75}$ can reach to −1623 ppm. These results should be useful for the quest of better magnetostrictive materials.

We further extended our investigations to alloys with other 5d elements such as Ir, Os, and W, as well as other metalloid elements such as Al, Si, and Zn. In Table I, one can see that many of these hypothetical alloys have giant magnetostriction: $|\lambda_{001}| > 1000$ ppm. We used the $B2$-like and $D0_3$-like structures in a 16-atom unit cell for these calculations. Both structures are stable under tetragonal distortions, except the $D0_3$-like structure in $Fe_{87.5}Pt_{6.25}Ga_{6.25}$. Large magnetostriction was mostly found in the $B2$-like structure but it is not necessary to be energetically preferential for some alloys studied here. It is known that the magnetostriction of Fe-based alloys is not necessary from the ground-state geometries. Although atomic models in the present work might be too simple to represent complex ternary alloys, the predicted large magnetostriction appears to be robust and attainable. We believe that rationally mixing 5d and metalloid elements into Fe is conceptually a good strategy for the fabrication of strong magnetostrictive materials. More extensive investigations on the atomic distribution and the effect on magnetostriction of ternary alloys, including thermodynamic stabilities of different phases, will be performed in the future with larger unit cells to provide insights for the experimental work.

TABLE I. Calculated slopes of $E_{MCA}(\varepsilon)$ curves, shear moduli, and values of λ_{001} of various Fe-based alloys.

FeX	$dE_{MCA}/d\varepsilon$ (meV)	Shear modulus C' (GPa)	λ (ppm)
$Fe_{87.5}Pt_{6.25}Al_{6.25}$	196.4	31.3	1156
$Fe_{87.5}Pt_{6.25}Ga_{6.25}$	175.6	34.1	943
$Fe_{75}Pt_{6.25}Si_{18.75}$	−164	21.7	−1623
$Fe_{75}Pt_{6.25}Ga_{18.75}$	13.2	10.7	222
$Fe_{75}Pt_{6.25}Ge_{18.75}$	−164.5	8.9	−3553
$Fe_{75}Pt_{6.25}Zn_{18.75}$	36.8	16.1	431
$Fe_{75}Ir_{6.25}Al_{18.75}$	−103.9	16.1	−1199

IV. CONCLUSIONS

In conclusion, we performed systematic density functional calculations on the magnetostriction of Fe-based alloys with the addition of 5d elements. The theoretical results indicate that many model systems may have giant magnetostrictive coefficients, $|\lambda_{001}| > 1000$ ppm, and hence are potentially useful for practical applications. Detailed analyses on the electronic origins demonstrated that the effective combination of large spin-orbit coupling of heavy elements, strong spin polarization of Fe, nonbonding states around the Fermi level, and adjustable number of electrons, are of great importance to improve magnetostriction of transition-metal systems. This provides an instructive guideline for the design of magnetostrictive materials.

ACKNOWLEDGMENTS

The authors thank A. E. Clark, K. B. Hathaway, and M. Wun-Fogle for insightful discussions. Work was supported by the ONR under Grant No. N00014-08-1-0143. Calculations were performed on the DoD supercomputers.

[1] B. Sanyal, C. Antoniak, T. Burkert, B. Krumme, A. Warland, F. Stromberg, C. Praetorius, K. Fauth, H. Wende, and O. Eriksson, Phys. Rev. Lett. **104**, 156402 (2010).
[2] K. Sato and H. Katayama-Yoshida, Semicond. Sci. Technol. **17**, 367 (2002).
[3] M. Weisheit, S. Fähler, A. Marty, Y. Souche, C. Poinsignon, and D. Givord, Science **315**, 349 (2007).
[4] T. A. Lograsso and E. M. Summers, Mater. Sci. Eng., A **416**, 240 (2006).
[5] E. M. Summers, T. A. Lograsso, and M. Wun-Fogle, J. Mater. Sci. **42**, 9582 (2007).
[6] D. Chiba, M. Yamanouchi, F. Matsukura, and H. Ohno, Science

301, 943 (2003).
[7] D. Chiba, M. Sawicki, Y. Nishitani, Y. Nakatani, F. Matsukura, and H. Ohno, Nature (London) **455**, 515 (2008).
[8] R. Ramesh and N. A. Spaldin, Nature Mater. **6**, 21 (2007).
[9] C. W. Nan, M. I. Bichurin, S. X. Dong, D. Viehland, and G. Srinivasan, J. Appl. Phys. **103**, 031101 (2008).
[10] A. E. Clark, M. Wun-Fogle, J. B. Restorff, T. A. Lograsso, and J. R. Cullen, IEEE Trans. Magn. **37**, 2678 (2001).
[11] J. R. Cullen, A. E. Clark, M. Wun-Fogle, J. B. Restorff, and T. A. Lograsso, J. Magn. Magn. Mater. **226-230**, 948 (2001).
[12] R. Q. Wu, J. Appl. Phys. **91**, 7358 (2002).
[13] S. Bhattacharyya, J. R. Jinschek, A. Khachaturyan, H. Cao, J. F. Li, and D. Viehland, Phys. Rev. B **77**, 104107 (2008).
[14] H. Cao, P. M. Gehring, C. P. Devreugd, J. A. Rodriguez-Rivera, J. Li, and D. Viehland, Phys. Rev. Lett. **102**, 127201 (2009).
[15] Y. N. Zhang, J. X. Cao, and R. Q. Wu, Appl. Phys. Lett. **96**, 062508 (2010).
[16] L. Dai, J. Cullen, M. Wuttig, T. A. Lograsso, and E. Quandt, J. Appl. Phys. **93**, 8627 (2003).
[17] A. E. Clark, J. B. Restorff, M. Wun-Fogle, K. B. Hathaway, T. A. Lograsso, M. Huang, and E. M. Summers, J. Appl. Phys. **101**, 09C507 (2007).
[18] J. X. Cao, Y. N. Zhang, W. J. Ouyang, and R. Q. Wu, Phys. Rev. B **80**, 104414 (2009).
[19] E. Wimmer, H. Krakauer, M. Weinert, and A. J. Freeman, Phys. Rev. B **24**, 864 (1981); M. Weinert, E. Wimmer, and A. J. Freeman, *ibid.* **26**, 4571 (1982).
[20] R. Q. Wu and A. J. Freeman, J. Magn. Magn. Mater. **200**, 498 (1999).
[21] J. P. Perdew, K. Burke, and M. Ernzelhof, Phys. Rev. Lett. **77**, 3865 (1996).
[22] D. S. Wang, R. Q. Wu, and A. J. Freeman, Phys. Rev. B **47**, 14932 (1993).
[23] Y. Mokrousov, G. Bihlmayer, S. Heinze, and S. Blugel, Phys. Rev. Lett. **96**, 147201 (2006).
[24] J. H. Wang, C. S. Jo, and R. Q. Wu, Appl. Phys. Lett. **92**, 032507 (2008).
[25] T. Burkert, L. Nordstrom, O. Eriksson, and O. Heinonen, Phys. Rev. Lett. **93**, 027203 (2004).
[26] D. Weller, A. Moser, L. Folks, M. E. Best, W. Lee, M. F. Toney, M. Schwickert, J.-U. Thiele, and M. F. Doerner, IEEE Trans. Magn. **36**, 10 (2000).
[27] Fe(C) denotes Fe atoms nearest to both Ga and Pt in the supercell.
[28] Y. N. Zhang, J. X. Cao, I. Barsukov, J. Lindner, B. Krumme, H. Wende, and R. Q. Wu, Phys. Rev. B **81**, 144418 (2010).
[29] The strain-induced shift of each state in Fig. 3 was obtained by fitting its eigenvalue ~ strain curve. The eigenvalues are measured from the Fermi level.
[30] The calculated E_{MCA}-N_e curves of $Fe_{75}Pt_{6.25}Ge_{18.75}$ overlap very well with the corresponding results of $Fe_{75}Pt_{6.25}Ga_{18.75}$, indicating the applicability of our rigid-band analysis.
[31] A. E. Clark, J. P. Teter, and O. D. McMasters, J. Appl. Phys. **63**, 3910 (1988).